GLI1, a novel target of the ER stress regulator p97/VCP, promotes ATF6f-mediated activation of XBP1

Luciana L. Almada, Kim Barroso, Sandhya Sen, Murat Törüner, Ashley N Sigafoos, Glancis L Raja Arul, David R Pease, Renzo E. Vera, Rachel L O Olson, Holger W Auner, et al.

GLI1, a novel target of the ER stress regulator p97/VCP, promotes ATF6f-mediated activation of XBP1

Luciana L. Almada[1,#], Kim Barroso[1,2,3,#], Sandhya Sen[1], Murat Toruner[1], Ashley N. Sigafoos[1], Glancis L. Raja Arul[1], David R. Pease[1], Renzo E. Vera[1], Rachel L. O. Olson[1], Holger W. Auner[4], Rémy Pedeux[2,3], Juan L. Iovanna[5], Eric Chevet[2,3,*], Martin E. Fernandez-Zapico[1,*]

[1]Schulze Center for Novel Therapeutics, Division of Oncology Research, Department of Oncology, Mayo Clinic, Rochester, MN, USA. [2]INSERM U1242, "Oncogenesis, Stress, Signaling", Université de Rennes, Rennes, France. [3]Centre de Lutte Contre le Cancer Eugène Marquis, Rennes, France. [4]Imperial College London, London, UK. [5]Centre de Recherche en Cancérologie de Marseille (CRCM), INSERM U1068, CNRS UMR 7258, Aix-Marseille Université and Institut Paoli-Calmettes, Parc Scientifique et Technologique de Luminy, Marseille, France.

Running title: Role of the p97/GLI1 axis in ER stress response

Keywords: ER stress, UPR, p97/VCP, Hedgehog, GLI1, HDAC1, USF2

[#] Share Co-First Authorship

*Corresponding authors: Martin E. Fernandez-Zapico, Mayo Clinic, 200 First St. SW, Rochester, MN 55905. TEL : 1 (507-255-0285), Email: fernandezzapico.martin@mayo.edu; Eric Chevet, INSERM U1242, "Oncogenesis, Stress, Signaling", Université de Rennes, Rennes, France. TEL : 33 (2) 232-37258, Email: eric.chevet@inserm.fr

Abstract

Upon accumulation of improperly folded proteins in the Endoplasmic Reticulum (ER), the Unfolded Protein Response (UPR) is triggered to restore ER homeostasis. The induction of stress genes is a *sine qua non* condition for effective adaptive UPR. Although this requirement has been extensively described, the mechanisms underlying this process remain in part uncharacterized. Here, we show that p97/VCP, an AAA+ ATPase known to contribute to ER stress-induced gene expression, regulates the transcription factor GLI1, a primary effector of Hedgehog (Hh) signaling. Under basal (non-ER stress) conditions, GLI1 is repressed by a p97/VCP-HDAC1 complex while upon ER stress GLI1 is induced through a mechanism requiring both USF2 binding and increase histone acetylation at its promoter. Interestingly, the induction of GLI1 was independent of ligand-regulated Hh signaling. Further analysis showed that GLI1 cooperates with ATF6f to induce promoter activity and expression of XBP1, a key transcription factor driving UPR. Overall, our work demonstrates a novel role for GLI1 in the regulation of ER stress gene expression and defines the interplay between p97/VCP, HDAC1 and USF2 as essential players in this process.

Introduction

The Endoplasmic Reticulum (ER), the first compartment of the secretory pathway, is responsible for the proper folding, maturation, quality control and transport of secretory or transmembrane proteins. Thus, it plays a key role in the maintenance of cellular homeostasis [1]. Failure of an adequate protein folding and quality control, which is an error-prone process, can lead to proteotoxic stress and subsequent cell death [1]. In response to the accumulation of improperly folded proteins, a well-characterized pathway, the Unfolded Protein Response (UPR), is activated to restore ER homeostasis by increasing protein folding and clearance capacities [2]. UPR signaling includes the activation of transcription factors controlling the expression of stress response genes mainly encoding proteins essential for the recovery of homeostatic ER functions [1].

Herein, we present evidence for a novel role of AAA^+ ATPase (ATPases Associated with various cellular Activities) p97/VCP in the regulation of gene expression during ER stress. p97/VCP is a segregase extracting proteins from complexes, organelle membrane or chromatin to facilitate their recycling or degradation by the proteasome. p97/VCP dysregulation has been implicated in numerous pathological conditions including cancer, and it is now recognized as a suitable therapeutic target in translational oncology [3-5]. Beyond its global role in protein homeostasis [4, 5], p97/VCP in the ER has been associated with various mechanisms including membrane fusion and organelle biogenesis [6, 7, 8] or ER-associated degradation (ERAD) [9, 10]. Moreover, it has been demonstrated that p97/VCP is involved in the regulation of ER stress induced gene expression through specific mechanisms dependent on the other AAA+ ATPase RUVBL2 in both *C. elegans* and mammalian cell systems [11, 12]. We identified the transcription factor GLI1, a major effector of the Hedgehog (Hh) pathway implicated in the development of several cancers [13, 14], as one of the genes whose expression is regulated by p97/VCP during ER stress. Importantly, the regulation of GLI1 was independent of the Hh ligand but depended on USF2, a member of the bHLHZIP family of transcription factors [15]. Further, in cancer cells, we showed that GLI1 cooperates with ATF6f to activate the expression of XBP1, a central regulator of stress genes under ER homeostasis imbalance. Thus, our results define a novel pathway contributing to the

regulation of the cellular ER stress response by antagonizing p97/VCP via a non-canonical activation of the Hh pathway.

Results

p97/VCP acts as a repressor of GLI1

To identify genes that could be regulated by p97/VCP in cancer cells, we evaluated the expression of a subset of disease-relevant genes previously reported to be associated with the inhibition, changes in activity or dominant mutant of this AAA+ ATPase [16-18]. To this end, the expression of *BRCA1*, *EGFR*, *FGF2*, *FGF12*, *IGFR2*, and *GLI1* mRNA was investigated in cancer cells silenced for p97/VCP using two independent siRNA targeting sequences (**Fig. 1A, Fig. S1A**). Knockdown efficiency was evaluated using immunoblot and RT-qPCR (**Fig. 1A Inset, Fig. S1A**). This analysis showed that the expression of *EGFR*, *FGF2*, *FGF12*, *IGFR2*, and *GLI1* mRNAs was upregulated in p97/VCP silenced HeLa cells while the other p97/VCP target gene was not significantly altered (**Fig. 1A**). Because of the direct regulatory effect of GLI1 on survival [19, 21], a key cellular function regulated by ER stress response [13-15], we used it as model to further our understanding of the gene expression mechanism(s) controlling this stress response. Similar to the findings in HeLa cells, knockdown of p97/VCP in Huh7 and U87 cells (**Fig. 1B**) resulted in increased levels of GLI1. Immunoblot analysis shows the efficiency of the RNAi knockdown (**Fig. 1B Inset**).

Next, we examined the subcellular localization of p97/VCP using a fractionation approach followed by immunoblotting. Consistent with previous results [22], we found that p97/VCP localized to both cytosol and nucleus of HeLa and U87 cells (**Fig. S1B**) thus suggesting that this ATPase could potentially play a direct role in nuclear functions including the transcriptional regulation of GLI1. Further, chromatin Immunoprecipitation Assay (ChIP) showed binding of p97/VCP to the promoter of GLI1 in HeLa (**Fig.1C**) and U87 cells under basal conditions (**Fig. S1C**). This binding was decreased upon treatment with Tunicamycin (Tun) (a N-linked glycosylation inhibitor and a well-established ER stressor [23] (**Fig.1D**). As control for the ChIP specificity, we evaluated the presence of p97/VCP to gene desert regions [24-25]. Data included in **Fig. 1C, 1D**

and **Fig. S1C** showed no binding of p97/VCP to these genomic sequences under basal or ER stress conditions. Further, we demonstrated that GLI1 expression was induced upon Tun treatment (**Fig. 1E**) and showed an additive effect to the knockdown of p97/VCP at both mRNA and protein levels (**Fig. 1E**). Efficiency of the KD and Tun treatment and their effect on the expression of GLI1 was analyzed by immunoblotting (**Fig. 1E**, **right panel**). Finally, we evaluated whether the effect of Tun was shared with other known ER stressors (DL-Dithiothreitol (DTT) and Brefeldin A (BFA)) [26-28]. Data in **Fig. S1D** shows that upon treatment with those stressors the expression of GLI1 was not increased compared to Tun treatment, likely indicating that the activation of GLI1 might require specific ER stress dependent signaling networks that might be absent or altered upon DTT (e.g. disulfide dependent complexes) or BFA (e.g. trafficking from the ER to the Golgi complex). As control for the ER stressors treatment, we used the expression of XBP1s (spliced form) and XBP1u (unspliced form). The data included in **Fig. S1D** shows increased levels of these transcription factors upon treatment with DTT and BFA. These findings revealed that GLI1 is a transcriptional target of ER stress and that its upregulation requires p97/VCP inhibition, identifying it as a novel GLI1 repressor.

USF2 is required by ER stress response to induce GLI1 expression

In silico analysis of p97/VCP binding region in the *GLI1* promoter identified the transcription factor USF2 as a candidate mediator of the regulation of GLI1 under ER stress (**Fig. 2B, lower panel**). To test if USF2 controls the expression of GLI1 in HeLa and U87 cells, USF2 expression was knocked down by RNAi-mediated silencing. USF2 knockdown led to lower levels of GLI1 mRNA (**Fig. 2A**). These results were validated using a second USF2 siRNA targeting sequence (**Fig. S2A**). Next, we performed a ChIP assay on the *GLI1* promoter where *in silico* analysis predicted a candidate USF2 binding site. Our results showed that upon ER stress, USF2 binds to the *GLI1* promoter (**Fig. 2B**) and it is required by the ER stress response to induce the expression of this transcription factor in HeLa (**Fig. S2B**) and U87 cells (**Fig. 2C**). Finally, we demonstrated that the knockdown of p97/VCP increased the binding of USF2 to the *GLI1* promoter thereby phenocopying the treatment with Tun in HeLa and U87 cells (**Fig. S2C**).

Next, we evaluated whether the activation of GLI1 is mediated by Hh ligand-dependent activation of the pathway, To this end, cells were treated with Smoothened Agonist, SAG (a known agonist of this pathway [29]). Treatment of HeLa and U87 cells with SAG did not affect the expression of GLI1 as well as PTCH1, a commonly used marker for the activation of the pathway [30]. (**Fig. S3A**). As positive control for our studies was used the Hh ligand responsive 10T1/2 cell line [31]. As shown in **Fig. S3A** the agonist of Hh ligand induced the expression of both, GLI1 and PTCH1 in 10T1/2 cells. To confirm these results, we used Vismodegib (Vis), a pharmacological inhibitor preventing activation of the pathway by binding to the Smoothened receptor (SMO), the receptor driving the ligand-dependent activation of the Hh signaling [32]. After 48 h of treatment with Vis, GLI1 mRNA expression was not significantly altered comparing control (Bar1 vs. Bar2 **Fig. S3B**) to ER stressed cells (Bar 3 vs. Bar 4 **Fig. S3B**). This indicates that GLI1 mRNA induction during ER stress is independent of the Hh ligand. Evaluation of GLI1 target genes within the Hh pathway (HHIP, PTCH1) showed induction of these molecules upon Tun treatment (**Fig. S3C**). Further analysis showed that these cells do not have cilia which may explain SAG's lack of effect (**Fig. S3D**). It has been shown that cilia plays a key role for the ligand-dependent activation of the Hh pathway [33]. Together, these results suggest that an interplay between p97/VCP and the transcriptional activator USF2 regulates the expression of GLI1 mRNA during ER stress independently of the Hh ligand.

ER stress antagonizes a newly identified p97/VCP-HDAC1 complex and increases GLI1 promoter acetylation

We next aimed at investigating whether ER stress prompted the modification of the chromatin landscape of the *GLI1* promoter. Notably, ER stress induced the levels of histone acetylation marks associated with gene activation including H3K27Ac, H3K14Ac and H4Ac [9] (**Fig. 3A**) and, binding of p300, a histone acetyltransferase associated with USF2 activity [34, 35] (**Fig. 3B**). These results suggest that under basal conditions the removal or the lack of acetylation at the GLI1 gene may cause its repression, however ER stress promotes binding of USF2 and acetylation of the *GLI1* promoter leading to increased expression of this gene. Given the role of p97/VCP in the regulation HDAC1

expression [12] and its regulation of RUVBL2 (a known interactor of HDAC1 [36]), we tested whether HDAC1 was involved in the repression of GLI1 under non-ER stress conditions. Hence, under basal conditions HDAC1 is bound to the *GLI1* promoter in HeLa and U87 cells (**Fig. 3C**). Using a co-immunoprecipitation approach, we found that p97/VCP co-immunoprecipitated with HDAC1 in HeLa cells (**Fig. 3D**). Further, we demonstrated that binding of HDAC1 was reduced in cells treated with the ER stress inducer Tun (**Fig. 3E**). As such we propose that a repressor complex containing HDAC1 controls the expression of GLI1 under basal conditions, and that under ER stress is disrupted to allow the binding of USF2 and subsequent activation of GLI1 transcription.

GLI1 is a positive regulator of XBP1 expression under ER stress

We next sought to evaluate the relevance of GLI1 activation in the context of ER stress. Sequencing experiments unveiled that XBP1u (unspliced form of XBP1) was candidate target gene of GLI1 [37, 38]. This was further supported by a promoter analysis of XBP1 gene (**Fig. 4A, top panel**). We first demonstrated the presence of GLI1 at two regions in the *XBP1* promoter. Importantly, GLI1's binding was induced by Tun (**Fig. 4A, left bottom panels**). XBP1 expression is also known to be activated by ATF6f [39] and we found that both ATF6f (A) and GLI1 (G) binding sites were in very close proximity on the *XBP1* promoter (**Fig. 4A, top panel**). Interestingly, knockdown of GLI1 demonstrated its requirement for the binding of ATF6f induced by Tun (**Fig. 4A, right bottom panel**). In HeLa cells luciferase reporter assays show that the overexpression of GLI1 and ATF6f cooperate to increase *XBP1* promoter activity (**Fig. 4B**). Further, we demonstrated that GLI1 is required by ATF6f to regulate this promoter. Knockdown of GLI1 impaired ATF6f induction of *XBP1* promoter activity (**Fig. 4C**). Expression controls for the overexpression and knockdown efficacy were evaluated using immunoblot (**Fig. 4B** and **4C**, **lower panels**). This unveiled that on both sites and for both transcription factors, Tun enhanced binding to the promoter and GLI1 knockdown attenuated this response, thereby implying some cooperativity between both transcription factors. These observations were confirmed when we monitored mRNA expression of ATF6f targets, XBP1u and the subsequent IRE1-mediated XBP1s (spliced form), and showed that all were dependent on the presence of GLI1 for maximal

response to ER stress induction. Using two independent siRNA targeting GLI1 we showed that knockdown of this transcription factor impairs the XBP1u (and the subsequent XBP1s) induction by Tun (**Fig. 4D, Fig. S4A**). Together these results indicate that p97/VCP is at the center of an ER stress-regulated transcriptional mechanism that integrates a repressor complex (HDAC1) and at least two transcription factors (USF2 and GLI1) in order to achieve a full and sustained adaptive response through XBP1.

Discussion

In this study, we have shown that p97/VCP can interact in a stress dependent manner with signaling complexes that include HDAC1 to control gene expression of GLI1, a novel effector of ER stress gene transcription response. Our results demonstrate that under basal conditions, GLI1 and ER stress genes are repressed by chromatin complexes containing p97/VCP and HDAC1 and these are in line with our previous report demonstrating that p97/VCP interacts with and controls the expression of RUVBL2 [10]. Promoter deacetylation prevents access to the transcription machinery and therefore the transcription of the target genes [40]. Our results suggest that this repressor complex could be antagonized at the GLI1 promoter by USF2. Thus, allowing chromatin to be in an open state, a condition favorable for transcription activation. Overall, the expression of GLI1 and ER stress genes may be turned off by deacetylation under basal conditions, but upon ER stress they could be turned on through a p97/VCP-dependent mechanism that acts as a molecular switch by inactivating repressor complexes.

Although p97/VCP silencing leads to the stabilization of repressor molecules, it is also known to cause ER stress, through attenuation of ER-associated degradation [41] and to induce the expression of ER stress genes [19]. In the context of our model, this suggests that either the remaining pool of p97/VCP is sufficient to regulate ER stress genes and/or the cell can induce these genes by other mechanisms independent of p97/VCP-mediated extraction of ubiquitinylated of repressor molecules. As siRNA mediated knockdown is never fully effective it is conceivable that the remaining pool of p97/VCP is preferentially translocated to the nucleus where it could exert its functions to induce

transcription of ER stress genes. Additionally, in this scenario, decrease in cytosolic p97/VCP could impair the degradation of other ER stress regulators by the proteasome and explain its stabilization. An example of such an alternative mechanism has been described in yeast as the degradation of most nuclear ubiquitinylated proteins is mediated by the ubiquitin protein ligase San1 [42]. Moreover, Gallagher et al. showed that although San1 and the p97/VCP orthologue CDC-48 have common substrates, CDC-48 is not universally required for the degradation of ubiquitinylated nuclear proteins. Similarly, GLI1 is also induced upon p97/VCP silencing, although the mechanism described above might explain this phenotype, it is also possible that the accumulation of activators is responsible for GLI1 induction. Indeed, Smad2/3 are other transcription factors known to regulate GLI1 and they were recently demonstrated to interact with p97/VCP on chromatin regions corresponding to other genes [43]. As a result, it is probable that accumulation of USF2 and Smad2/3 is sufficient to induce GLI1 expression in p97/VCP-silenced cells. GLI1 in turn cooperates with ATF6f to induce the expression of a major effector of the UPR, XBP1u, thus adding to the previously reported action of ATF6f [44]. Since GLI1 is necessary for ATF6f binding on XBP1 promoter region, our work may unveil a key regulatory mechanism to sustain the expression of XBP1u, which together with IRE1 activation may lead to prolonged XBP1s expression. In addition, GLI1 is one of the main effectors of the Hh pathway. Activation of this pathway is suggested to participate to the pathogenesis of multiple malignancies [13, 14] and has also been associated with ER homeostasis maintenance [45-50]. Our results suggest now that upon ER stress GLI1 is activated, which leads to the non-canonical (ligand-independent) activation of the Hh pathway, a mechanism that might contribute to tumor initiation and progression. These observations provide some mechanistic details on how ER stress might contribute to the carcinogenesis, as previously reported [51].

Overall our work identifies p97/VCP as a molecular switch able to induce ER stress gene expression by inhibiting a repressor complex upon ER stress beyond its role in ER-associated degradation. We have discovered that this mechanism is not exclusive to ER stress genes. Indeed, ER stress also leads to the non-canonical activation GLI1 in a p97/VCP and HDAC1 complex-dependent manner and as a consequence to activation

of Hh genes. As p97/VCP inhibition was described to induce Epithelial to Mesenchymal Transition (EMT)-like phenotypes [52] and also to contribute to the activation of pro-oncogenic genes (GLI1, the present study), the potential use of p97/VCP pharmacological inhibitors in neoplastic diseases needs to be carefully considered.

Materials and Methods

Antibodies, Plasmids, Cell lines and Reagent - Western blotting was performed using the following antibodies: anti-GLI1 (Cell Signaling Technology, 3538), anti-FLAG (Sigma-Aldrich, F1804), anti-Lamin A (Abcam, ab26300), anti-GAPDH (GeneTex, GTX627408), anti-Actin (Sigma- Aldrich, A5441), anti-p97/VCP (Proteintech, 60316-1 and 10736-1-AP), anti-HDAC 1 (Cell Signaling Technology, 9928); anti-ATF6f (Active Motif, 40962) and anti-Tubulin (Sigma, T9026). For ChIP experiments, the following antibodies were used: anti-p97/VCP (Proteintech, 60316-1); anti-USF2 (Santa Cruz, sc-862 and sc-518074); anti-GLI1 (Novus, NB600-600); antibody against H3K14Ac, H3K27Ac, normal rabbit IgG and normal mouse IgG were from Abcam (ab52946, ab4729, ab37415 and ab18413), anti- H4Ac (Millipore, 06-598) ; anti-ATF6f (Active Motif, 40962); anti-p300 (Abcam, ab14984) and anti-HDAC1 (Cell Signaling Technology, 9928). Tunicamycin (Tun) was from Calbiochem (EMD Millipore, 654380). Brefeldin A (BFA) was purchased from Invitrogen (00-4506-51) and, DL-Dithiothreitol (DTT) from Sigma Aldrich (D0632). Smoothened Agonist (SAG)-HCl (S7779) and Vismodegib (Vis, GDC-0449) were from Selleckchem. The magnetic beads used for the co-immunoprecipation and ChIP assays were purchased from Life technologies (Dynabeads, 10006D and 10007D). The reporter plasmid pGL3-Basic was linearized using restriction enzymes KpnI and HindIII, the 4,770 bp vector was gel purified. Primers 5'-GAACATTTCTCTATCGATAGGTACCGGCCCAAGCTGATGAGAGT-3' and 5'-GTTTTTGGCGTCTTCCATGGTGGCAGCTCCAGACTACGCACCG-3' were used to amplify the 2,039 bp XBP1 promoter region (-1 to -1944) from gDNA of HPNE cells [22]. The pGL3-Basic vector and XBP1 promoter fragment were then cloned together via Gibson Assembly protocol. The ATF6-FLAG and GLI1-FLAG constructs were previously described [7, 23]. HeLa, U87 and Huh7 were cultured in DMEM from Life Technologies (41965) supplemented with 10% FBS from Sigma-Aldrich (12003C). 10T1/2 cells were grown in BME (Gibco, 21010046) supplemented with 2 mM L-glutamine (Gibco, 1117210) and 10% FBS. All cell cultures were maintained in a 37°C incubator containing 5% CO_2.

For knockdown studies, siRNAs were purchased from Dharmacon, ON-TARGETplus siRNA system (siGLI1#2, J-0033896-06-0005 and NT, D-001810-10-20) and from QIAGEN, FlexiTube siRNA system (siGLI1, SI03063641; sip97/VCP, SI03019681; sip97/VCP#2, SI03019730; siUSF2, SI00051345; siUSF2#2, SI02780785; NT, AllStars Negative control, 1027281).

Cell treatments – For Tunicamycin, cells were treated for 6 h or 24 h with 5 μg/ml Tun in complete growth medium. For Brefeldin A, cells were treated with 3 μg/ml BFA for 4 h or 24 h in complete growth medium. For DL-Dithiothreitol, cells were treated for 24 h with 3 mM DTT in complete growth medium. For Smoothened Agonist HCl, cells were incubated in serum-free media overnight, followed by 24 h incubation with 5 nM SAG in serum-containing growth medium. For Vismodegib cells were treated with 1 μM Vis for 48 h.

Real Time-Quantitative PCR (RT-qPCR) - Total RNA was extracted using Trizol reagent (Invitrogen, 15596018) following the manufacture's protocol. For the Reverse Transcription 2 μg of mRNA were used with the High-Capacity cDNA Reverse Transcription Kit (Thermo Fisher Scientific, 4368813). A portion of the total cDNA was amplified by real-time PCR. Samples were prepared with iTaq™ Universal SYBR® Green Supermix (Bio-Rad, 1725274) and the following primers: GLI1, 5′-TTCCCAACTTGCCAGCTGAA-3′ (sense) and 5′-ACAGGGGATCCTGTATGCCT-3′ (antisense);BRCA1, 5'-GTGTCCAACTCTCTAACCTTGG-3' (sense) and 5'-TTGATCTCCCACACTGCAATAA-3' (antisense); EGFR, 5'-GCCTCCAGAGGATGTTCAATAA-3' (sense) and 5'-TGAGGGCAATGAGGACATAAC-3' (antisense); FGF2, 5'-GACCCTCACATCAAGCTACAA-3' (sense) and 5'-AGCCAGTAATCTTCCATCTTC-3' (antisense); FGF12, 5'-CAGCGACTACACTCTCTTCAATC-3' (sense) and 5'-TCACCATTCATGGCCACATAG-3' (antisense); IGFR2, 5'-ATCATTCAGTGGGTGACTCTG-3' (sense) and 5'-TGCTCTGGACTCTGTGATTTG-3' (antisense); p97/VCP, 5'-CCATCCGGAAAGGAGACATTT-3' (sense) and 5'-GTCTGGAGCAACAATGCAATAAG-3' (antisense); USF2, 5'-TTCGGCGACCACAACATCCAG-3' (sense) and 5'-

CAGTCACCTGGACTACGCGGT-3' (antisense); XBP1s, 5'-CGGAAGCCAAGGGGAATGAA-3' (sense) and 5'-GCAGAGGTGCACGTAGTCTG-3' (antisense); XBP1s, 5'-GCTGAGTCCGCAGCAGGT-3' (sense) and 5'-CTGGGTCCAAGTTGTCCAGAAT-3' (antisense); PTCH1, 5'-GTTGTGGGCCTCCTCATATT-3' (sense) and 5'-GACTTACTCGTCCTCCAACTTC-3' (antisense); HHIP, 5'-AGAACTGCAAAATGTGAGCCAG-3' (sense) and 5'-TCTGATCAAGAATACCTGCCCTG-3' (antisense); TBP, 5′-GGTTTGCTGCGGTAATCATGA-3′ (sense) and 5′-CTCCTGTGCACACCATTTTCC-3′ (antisense); HPRT, 5′-TGGAAAAGCAAAATACAAAGCCTAAGATGA-3′ (sense) and 5′-ATCCGCCCAAAGGGAACTGATAGTC-3′ (antisense); mouse GLI1, 5′-GCCACACAAGTGCACGTTTGA-3′ (sense) and 5′-GCTCACACATGTAAGGCTTCTCAC-3′ (antisense); mouse PTCH1, 5′-GCAGATTTCCAAGGGGAAGGC-3′ (sense) and 5′-CACAGCGAAGGCCCCAAATA-3′ (antisense); mouse PRT, 5′-AAGTGTTTATTCCTCATGGACTGA-3′ (sense) and 5′-CTCCCATCTCCTTCATGACATC-3′ (antisense); mouse TBP, 5′-GAAGTTCCCTATAAGGCTGGAAG-3′ (sense) and 5′-AGGAGAACAATTCTGGGTTTGA-3′ (antisense). Quantitative PCR was performed in a CFX384 Touch Real-Time PCR Detection System (Bio-Rad). . Each mRNA level was normalized by comparison with GAPDH or HPRT and TBP RNA levels in the same sample. The results were calculated following the 2ΔCp method. .

Small interfering RNA (siRNA) - siRNA used in this study were transfected into the cells by using Lipofectamine RNAiMAX (Invitrogen, 13778500) or DharmaFECT Transfection Reagent (Dharmacon, T-2001-03) according to the manufacturer's protocols. Cells were used for the experiments 48 h post-transfection.

Cell fractionation, and Co-immunoprecipitation analyses - For the cellular fractionation, HeLa, and U87 cell lines were plated at 3.5 X 10^6 and 4.0 X 10^6 cells in 15 cm2 dish, respectively. Next day cells were treated with Tun at concentration of 5 µg/ml. After 24 h of treatment cells were washed twice with chilled 1X PBS and harvested. For fractionation cells were lysed for 10 min on ice in CSK I buffer (10 mM PIPES pH

6.8,100 mM NaCl, 100 mM Sucrose, 1 mM MgCl2, 1 mM EDTA, 0.5% Triton X 100, 1 mM DTT, and 1x Protease inhibitor (Roche Applied Science, 11836170001), and centrifuged for 17,000 X *g* for 5 min. Supernatant was collected as a cytosolic fraction. The pellet contains the nucleus was washed twice with CSK I buffer then suspended in CSK II buffer (10 mM PIPES pH 6.8, 50 mM NaCl, 300 mM Sucrose, 6 mM MgCl2, 1 mM DTT, 1x Protease inhibitor, 40 U DNAse 1, and 1 X DNAse buffer) and incubated at 37°C for 20 min. For salt extraction of nuclear proteins $(NH4)_2SO4$ was added to a final concentration of 260 mM and incubated further at 37°C for 10 min. Sample were centrifuged at 17,000 X *g* for 2 min and supernatant was collected as nuclear fraction. Quantification of the protein was performed using a BCA-based kit with a BSA standard curve (Thermo Fisher Scientific, J63283.QA).

For co-immunoprecipitations, after a cold PBS wash cells were lysed with lysis buffer containing 30 mM Tris-HCL, pH 7,5, 150 mM NaCl and 1,5% CHAPS (Calbiochem) and Protease and Phosphatase inhibitors from Roche (05892791001, 04906837001). Supernatant were recovered following centrifugation at 17,000 X *g* for 15 min at 4°C and incubated overnight with the adequate antibody. Magnetic beads after 3 washes in the lysis buffer were added to the immune complexes for 20 min at RT with gentle rotation followed by washing 3 times in the lysis buffer. Immunoprecipitated proteins were resolved on 8 to 15% polyacrylamide gels and transferred to nitrocellulose or PVDF membranes (Thermo Fisher Scientific, 88018). Following this, membranes were blocked using PBS, 0.5% Tween20 (PBS-T) and 3% Bovine Serum Albumin for 30 min at room temperature. Primary antibodies were incubated with the membrane (ad-hoc dilution with PBS-T) for 12-16 h at 4°C. Membranes were then washed extensively with PBS-T prior incubation for 30 min at room temperature with HRP-conjugated secondary antibodies (depending on the primary) at a 1/7000 dilution.

Immunoblotting - Cells were washed twice with chilled 1X PBS then and lysed in RIPA buffer (50 mM Tris, pH 7.5, 150 mM NaCl, 5mM EDTA, 0.5% sodium deoxycholate, 1% NP-40, 0.1% SDS, 1 mM PMSF, and Complete protease inhibitor cocktail). The sample was passed for 10 times through 27 ½ gauze needle. Protein concentrations of lysates were determined using the BCA protein reagent (Thermo Fisher Scientific, J63283.QA).

Lysates were then denatured in Laemmli buffer with 0.5 % BME and ran on 4 to 15 % Bio-Rad Min-Protean TGX precast gels. Gels were transferred to PVDF membranes in Towbin transfer buffer with 0.01% SDS. The transferred membranes were blocked in 3% BSA in PBS with 0.1% Tween-20 (TBS-T) for 1 h. Membranes were then incubated at 4°C for overnight with primary antibodies in TBS-T with 3% BSA. Then, blots were incubated with HRP-conjugated secondary antibodies for 1 h at RT and immunoreactive signals on blots were detected with SuperSignal West Pico Chemiluminescent Substrate (Thermo Fisher Scientific, 34080). Signals were captured using a Chem-Doc imaging system (Bio-Rad).

Chromatin Immunoprecipitation – ChIPs were conducted as previously described [22]. Briefly, after Tun treatment, cells ($15x10^6$) were cross-linked with 1% formaldehyde, followed by cell lysis. DNA was sheared and aliquots of the sheared chromatin were then immunoprecipitated using magnetic beads and corresponding antibodies. Following immunoprecipitation, cross-links were removed, and immunoprecipitated DNA was purified using spin columns and subsequently amplified by quantitative PCR. PCR primers were designed to amplify a region of the GLI1 promoter containing potential USF2 binding sites and, regions of the XBP1 promoter containing potential GLI1 and/or ATF6f biding sites. The sequences of the primers were as follows: GLI1 promoter: 5′-TGAGGGAGGATGCTTAGGGG-3’ (sense); 5′-GGTCAAGAGATTGAGACCATCC-3’ (antisense); XBP1 promoter: Site 1: 5’-TAAATCGCTCCCGTGCTGC-3’ (sense);5’-GCGCCCAGCCTCTTGTTATT-3’ (antisense); Site 2; 5’-GGCCCAAGCTGATGAGAGTT-3’ (sense); 5’-TTGGAAAAGAGGTGGGGGTG-3’ (antisense)Samples for quantitative SYBR PCR were performed in triplicate using the CFX384 Touch Real-Time PCR Detection System. Results are represented as Percentage of Input or Fold of Enrichment as stated in the legends of figures.
For the chromatin preparation step, DNA was sheared as follow: Hela cells, by sonication (50 cycles) using a Bioruptor 300 (Diagenode); U87 cells, by digestion using MNase (312 U per 10^6 cells; ; New England BioLabs, M0247S).

Luciferase Reporter Assay - For Luciferase assay HeLa and U87 cells were seeded in triplicate at 0.25 X 10^5, 0. 50 X 10^5 cells per well in 12 well plate respectively. Next day, cells were co-transfected with XBP1 reporter and either pCMV, GLI1-FLAG, ATF6-FLAG constructs or their combination. After 24 h of transfection cells were lysed in passive lysis buffer (Promega, E1941) and luciferase assay was performed as per the manufacturer protocol (Promega, E1501). To normalize the light units, protein from each well was quantified using Bradford assay (Bio-Rad, 5000006). Relative luciferase units represent the luciferase/protein concentration readouts normalized to control group within each experiment.

Immunofluorescence - Cells plated on coverslips were washed once in 1x PBS followed by fixation in 3.6% paraformaldehyde for 10 minutes at room temperature. Cells were washed once post fixation with 1x PBS. Cells were then permeabilized in 0.1% Triton-X 100 at room temperature for 10 minutes. Cells were blocked with blocking buffer (4% bovine serum albumin in PBS) for 1 hour at room temperature. Cells were then incubated in 1^{α} antibody (1:200 anti-Acetylated α-Tubulin, Sigma Aldrich, Cat no. T6793; 1:200 Anti-γ-Tubulin, Sigma Aldrich, Cat no. T5326) in blocking buffer for 1 hour at room temperature. Cells were then washed in blocking buffer three times for 5 minutes at room temperature. Cells were incubated in 2^{α} antibody (1:1000 Alexa Fluor 594 goat anti-mouse IgG2b Invitrogen, Cat no. A21145; 1:1000 Alexa Fluor 488 goat anti-mouse IgG1 Invitrogen, Cat no. A21121) for 20 minutes at room temperature. Cells were then washed in 1x PBS three times for 5 minutes at room temperature. Coverslips were mounted on slides using ProLong™ Gold Antifade Mountant with DAPI (Invitrogen, Cat no. P36931). Mountant was allowed to cure for 24 hours before imaging. Cells were imaged on Ziess LSM 800 confocal microscope.

Statistical analysis - Evaluation of significance between two groups was done employing Student t-test or Mann-Whitney test in the case of non-parametric data. Difference between three or more groups was tested by one-way analysis of variance (ANOVA) with Dunnet post-hoc test. Statistical analysis was done using GraphPad Prism 9 software. All the results are expressed as mean ± standard error of at least

three independent experiments, and $P<0.05$ was considered statistically significant. References of figures: $P<0.05$ = *; $P<0.01$ = **; $P<0.001$ = ***; $P<0.0001$ = ****.

Abbreviations

ER: Endoplasmic Reticulum

AAA^+ ATPase: ATPases Associated with various cellular Activities

ChIP: Chromatin immunoprecipitation

Hh: Hedgehog

PBS-T: PBS, 0.3 % Tween 20

SE: standard error

Acknowledgements

We thank the Biosit histopathology H2P2 platform (https://histopathologie.univ-rennes.fr/ Université de Rennes, France) for help with immunocytochemistry and G. Jégou for technical support. We would like to thank Emily Porcher and Terry Stephenson for their secretarial assistance.

Funding and additional information

This work was funded by grants from INSERM, Institut National du Cancer (INCa; PLBio 2017, 2019, 2020), Région Bretagne, Rennes Métropole, Fondation pour la recherche Médicale (FRM ; DEQ20180339169), EU H2020 MSCA ITN-675448 (TRAINERS), la Ligue Contre le Cancer Comités d'Ille-et-Vilaine, des Côtes d'Armor et du Morbihan and MSCA RISE-734749 (INSPIRED) to EC and MEFZ was supported by NCI CA136526. KB was funded by a grant from la Ligue Contre le Cancer. The content of this manuscript is solely the responsibility of the authors and does not necessarily represent the official views of the National Institutes of Health or INSERM.

Competing interests

EC is a founding member of Thabor Tx (https://www.thabor-tx.com/). The other authors declare that they have no competing interests with the contents of this article.

Data Availability

All the data described are contained within the manuscript.

References

1. Hetz, C., E. Chevet, and S.A. Oakes, Proteostasis control by the unfolded protein response. Nat Cell Biol, 2015. **17**(7): p. 829-38.
2. Walter, P. and D. Ron, The unfolded protein response: from stress pathway to homeostatic regulation. Science, 2011. **334**(6059): p. 1081-6.
3. Kilgas S., Ramadan K. Inhibitors of the ATPase p97/VCP: From basic research to clinical applications. Cell Chem Biol, 2023. **30**(1): p. 3-21.
4. Dargemont C., Ossareh-Nazari B. Cdc48/p97, a key actor in the interplay between autophagy and ubiquitin/proteasome catabolic pathways. Biochim Biophys Acta, 2012. **1823**(1): p. 138-44.
5. Fessart D., et al. P97/CDC-48: proteostasis control in tumor cell biology. Cancer Lett, 2013. **337**(1): p. 26-34.
6. Baur T., Ramadan K., Schlundt A., Kartenbeck J., Meyer H.H. NSF- and SNARE-mediated membrane fusion is required for nuclear envelope formation and completion of nuclear pore complex assembly in Xenopus laevis egg extracts. J Cell Sci, 2007. **120**(Pt 16): p. 2895-903.
7. Latterich M. p97 adaptor choice regulates organelle biogenesis. Dev Cell, 2006. **11**(6): p. 755-7.
8. Lavoie C., Chevet E., Roy L., Tonks N.K., Fazel A., Posner B.I., Paiement J., Bergeron J.J. Tyrosine phosphorylation of p97 regulates transitional endoplasmic reticulum assembly in vitro. Proc Natl Acad Sci U S A, 2000. **97**(25): p. 13637-42.
9. Wu X., Rapoport T.A. Mechanistic insights into ER-associated protein degradation. Curr Opin Cell Biol, 2018. **53**: p. 22-28.
10. Meyer, H., et al. Emerging functions of the VCP/p97 AAA-ATPase in the ubiquitin system. Nat Cell Biol. 2012. **14**(2): p. 117-23.
11. Caruso, M.E., et al., GTPase-mediated regulation of the unfolded protein response in Caenorhabditis elegans is dependent on the AAA+ ATPase CDC-48. Mol Cell Biol, 2008. **28**(13): p. 4261-74.
12. Marza, E., et al., Genome-wide screen identifies a novel p97/CDC-48-dependent pathway regulating ER-stress-induced gene transcription. EMBO Rep, 2015.**16**(3): p. 332-40.
13. Tolosa E.J., et al. GLI1/GLI2 functional interplay is required to control Hedgehog/GLI targets gene expression. Biochem J. 2020 **477**(17):3131-3145.
14. Carpenter, R.L. and H.W. Lo, Hedgehog pathway and GLI1 isoforms in human cancer. Discov Med., 2012 **13**(69): p. 105-13.
15. Ghirlando R., et al., Chromatin domains, insulators, and the regulation of gene expression. Biochim Biophys Acta. 2012. **1819**(7): p. 644-51.
16. Nalbandian A, et al. Global gene profiling of VCP-associated inclusion body myopathy. Clin Transl Sci. 2012. 5(3):226-34.
17. Zhang Z, et al. Ter94 ATPase complex targets k11-linked ubiquitinated ci to proteasomes for partial degradation. Dev Cell. 2013. **25**(6):636-44.
18. Vekaria PH, et al. Functional cooperativity of p97 and histone deacetylase 6 in mediating DNA repair in mantle cell lymphoma cells. Leukemia. 2019. **33**(7):1675-1686.
19. Bastola P., et al. VCP inhibitors induce endoplasmic reticulum stress, cause cell cycle arrest, trigger caspase-mediated cell death and synergistically kill ovarian cancer cells in combination with Salubrinal. Mol Oncol. 2016. **10**(10):1559-1574.

20. Nishimura N., et al. Novel p97/VCP inhibitor induces endoplasmic reticulum stress and apoptosis in both bortezomib-sensitive and -resistant multiple myeloma cells. Cancer Sci. 2019. **110**(10):3275-3287.
21. Chou T.F., et al. Reversible inhibitor of p97, DBeQ, impairs both ubiquitin-dependent and autophagic protein clearance pathways. Proc Natl Acad Sci U S A. 2011. **108**(12):4834-9.
22. Almanza A., et al. Endoplasmic reticulum stress signalling - from basic mechanisms to clinical applications. FEBS J, 2019. **286**(2):241-278.
23. da Silva D.C., et al. Endoplasmic reticulum stress signaling in cancer and neurodegenerative disorders: Tools and strategies to understand its complexity. Pharmacol Res. 2020. **155**:104702.
24. Alexiadis V., et al. RNAPol-ChIP analysis of transcription from FSHD-linked tandem repeats and satellite DNA. Biochim Biophys Acta. 2007. **1769**: p. 29–40.
25. Shi Z., et al. SOX9 directly regulates IGFBP-4 in the intestinal epithelium. Am J Physiol Gastrointest Liver Physiol. 2013. **305**: p. G74–G83.
26. Shinjo S., et al. Comparative Analysis of the Expression Patterns of UPR-Target Genes Caused by UPR-Inducing Compounds. Biosci. Biotechnol. Biochem.2013. **77**(4): p. 729–735.
27. Proulx-Bonneau S., et al. A role for MT1-MMP as a cell death sensor/effector through the regulation of endoplasmic reticulum stress in U87 glioblastoma cells. J Neurooncol. 2011. **104**: p. 33–43
28. Epple L. Induction of the Unfolded Protein Response Drives Enhanced Metabolism and Chemoresistance in Glioma Cells. PLOS ONE. 2013. 8(8): e73267.
29. Chen J.K., et al. Small molecule modulation of Smoothened act. Proc Natl Acad Sci U S A 2002. **99(22)**:14071-6.
30. Sigafoos A.N., et al. Hedgehog/GLI Signaling Pathway: Transduction, Regulation, and Implications for Disease. Cancers (Basel), 2021. **13(14)**:3410.
31. Ingram W.J., et al. Novel genes regulated by Sonic Hedgehog in pluripotent mesenchymal cells. Oncogene, 2002. **21(53)**: p. 8196-205
32. Migden M., et al., A Review of Hedgehog Inhibitors Sonidegib and Vismodegib for Treatment of Advanced Basal Cell Carcinoma. J Drugs Dermatol. 2021. **20**(2):156-165.
33. Robbins DJ, et al. The Hedgehog Signal Transduction Network. Sci Signal. 2012. **5** (246), re6.
34. Breen G.A., and Jordan E.M. Transcriptional activation of the F(1)F(0) ATP synthase alpha-subunit initiator element by USF2 is mediated by p300. Biochim Biophys Acta. 1999. **1428**(2-3):169-76.
35. Green M, Panesar NK, Loewenstein PM. The transcription-repression domain of the adenovirus E1A oncoprotein targets p300 at the promoter. Oncogene. 2008. **27**(32):4446-55.
36. Kim J.H., et al. Roles of sumoylation of a reptin chromatin-remodelling complex in cancer metastasis. Nat Cell Biol, 2006. **8(6)**: p. 631-9.
37. Villavicencio, E.H., et al., Cooperative E-box regulation of human GLI1 by TWIST and USF. Genesis. 2002. **32**(4):247-58.
38. Peterson, K.A., et al., Neural-specific Sox2 input and differential Gli-binding affinity provide context and positional information in Shh-directed neural patterning. Genes Dev. 2012. **26**(24):2802–2816.

39. Yoshida, H., et al., XBP1 mRNA is induced by ATF6 and spliced by IRE1 in response to ER stress to produce a highly active transcription factor. Cell. 2001. **107**(7): p. 881-91.
40. Thiagalingam, S., et al., Histone Deacetylases: Unique Players in Shaping the Epigenetic Histone Code. Ann N Y Acad Sci. , 2003. **983**: p. 84-100.
41. Wu X, Rapoport TA. Mechanistic insights into ER-associated protein degradation. Curr Opin Cell Biol. 2018. **53**: p. 22-28.
42. Higgins, R., et al., The Cdc48 Complex Alleviates the Cytotoxicity of Misfolded Proteins by Regulating Ubiquitin Homeostasis. Cell Rep, 2020. **32**(2): p. 107898.
43. Ndoja, A., R.E. Cohen, and T. Yao, Ubiquitin signals proteolysis-independent stripping of transcription factors. . Mol Cell. 2014. **53**(6): p. 893-903.
44. Yoshida H., et al. XBP1 mRNA is induced by ATF6 and spliced by IRE1 in response to ER stress to produce a highly active transcription factor. Cell, 2001. **107**(7): p. 881-91.
45. Fatima Rangwala F., et al. Increased production of sonic hedgehog by ballooned hepatocytes. J Pathol, 2011. **224**(3): p. 401-10.
46. Marada S., et al. The unfolded protein response selectively targets active smoothened mutants. Mol Cell Biol 2013. **33**(12): p. 2375-87.
47. Saito A., et al. Chondrocyte proliferation regulated by secreted luminal domain of ER stress transducer BBF2H7/CREB3L. Mol Cell. 2014. **53**(1): p.127-39.
48. Gagné-Sansfaçon J., et al. Loss of Sonic hedgehog leads to alterations in intestinal secretory cell maturation and autophagy. PLoS One. 2014. **9**(6):e98751.
49. Bufalieri F., et al. ERAP1 promotes Hedgehog-dependent tumorigenesis by controlling USP47-mediated degradation of βTrCP. Nat Commun. 2019. **10**(1):3304.
50. Di Minin G., et al. TMED2 binding restricts SMO to the ER and Golgi compartments. PLoS Biol. 2022. **20**(3):e3001596.
51. Pommier, A., et al., Unresolved endoplasmic reticulum stress engenders immune-resistant, latent pancreatic cancer metastases. Science. 2018. **360**(6394): p. eaao4908.
52. Shah, P.P. and L.J. Beverly, Regulation of VCP/p97 demonstrates the critical balance between cell death and epithelial-mesenchymal transition (EMT) downstream of ER stress. Oncotarget. 2015. **6**(19): p. 17725-31.

Figure Legends

Figure 1: p97/VCP acts as repressor of GLI1 and antagonizes ER stress induction of GLI1 – A) RT-qPCR analysis of 6 cancer relevant genes (BRCA1, EGFR, FGF2, FGF12, IGFR2 and GLI1) in HeLa cells transfected with siRNA control (NT) or siRNA p97/VCP. Insert: western blotting confirming the KD of p97/VCP. β-Actin was run as loading control. **B)** RT-qPCR analysis of GLI1 expression in Huh7 and U87 cells after knockdown of p97/VCP. Insert: western blot confirming the KD of p97/VCP. β-Actin was run as loading control. **C)** ChIP assay performed in HeLa cells to analyze the binding of p97/VCP to the GLI1 promoter under basal conditions. A gene desert region on Chr12 (Gene desert) and an untranscribed region on Chr5 (Untr 5) were used as negative controls. **D)** ChIP assay performed in HeLa cells to analyze the binding of p97/VCP to the GLI1 promoter after treatment with Tun (5 μg/ml for 6 h). Untr 5 and Gene desert regions were used as negative controls. **E)** RT-qPCR analysis in U87 cells for the expression of GLI1 after treatment with Tun alone or in combination with the KD of p97/VCP. Insert: western blot ran to confirm the KD of p97/VCP and its effect on the expression of GLI1 in combination with Tun treatment. Tubulin was ran as loading control. Blots presented are representative of three independent experiments. Results are represented as the average ± SEM of at least three independent experiments. *p<0.05; **p<0.01; ***p<0.001, ****p<0.0001.

Figure 2: USF2 is required by ER stress to induce GLI1 expression – A) RT-qPCR analysis of GLI1 mRNA expression in HeLa (left panel) and U87 (right panel) cells silenced or not for USF2. **B)** ChIP assay performed on HeLa cells after treatment with Tun (5 μg/ml for 24 h) or vehicle (DMSO) to analyze the effect on the biding of USF2 to the promoter of GLI1. Lower panel: schematic representation of the GLI1 gene promoter region with the USF2 predicted binding site and the position of the primers used for the ChIP assay. **C)** Left panel: RT-qPCR analysis of the expression of GLI1 after the silencing of USF2 in combination with Tun treatment (5 μg/ml for 24 h) performed in U87 cells. Right panel: RT-qPCR analysis confirming the efficiency of the KD of USF2 under

the conditions previously described. Results are represented as the average ± SEM of at least three independent experiments. *p<0.05; **p<0.01; ****p<0.0001.

Figure 3: ER stress antagonizes a newly identified p97/VCP-HDAC1 complex to increase GLI1 promoter acetylation – A) ChIP assay performed on HeLa cell lysates from cells treated with either 5 μg/ml of Tun or DMSO for 24 h to analyze the effect on the enrichment of histone activation marks (H3K14Ac, H3K27Ac and H4Ac) on the promoter of GLI1. **B)** ChIP assay performed on HeLa cell lysates from cells treated with either 5 μg/ml of Tun or DMSO for 24 h to analyze the binding of the histone acetyltransferase p300 on the same region of the GLI1 promoter. **C)** ChIP assay performed on HeLa and U87 cells to analyze the enrichment of the histone deacetylase HDAC1 on the promoter of GLI1 under basal conditions. **D)** Characterization of the association between p97/VCP and HDAC1 in HeLa cells. Lysates were immunoprecipitated with HDAC1 antibody and the immune complex immunoblotted using anti-p97/VCP, anti-HDAC1. **E)** ChIP assay performed on HeLa subjected to Tun treatment (5 μg/ml for 24 h) to study the effect on the enrichment of HDAC1 on the GLI1 promoter. Blots presented are representative of three independent experiments. Results are represented as the average ± SEM of at least three independent experiments. *p<0.05; **p<0.01; ***p<0.001.

Figure 4: ATF6f and GLI1 cooperate to promote XBP1 expression during ER stress – A) Top panel: schematic representation of the XBP1 gene promoter region with the two GLI1/ATF6f predicted binding sites and the position of the primers (1 and 2) used for the ChIP assay. Lower panel: ChIP assay performed on lysates from U87 cells transfected with siRNA targeting GLI1 or NT and treated with either 5 μg/ml of Tun or DMSO for 24 h. qPCR was performed to determine the effect of treatment on the biding of GLI1 (left) and ATF6f (right) to the XBP1 promoter. **B)** XBP1 promoter reporter activity evaluated in HeLa cells transfected with plasmids for empty vector (pCMV), GLI1 and/or ATF6f along with the XBP1 luciferase reporter. Lower panel: western blot confirming the overexpression of GLI1 and ATF6f. β-Actin was run as loading control. **C)** XBP1 promoter reporter activity evaluated in U87 cells transfected with siRNA targeting GLI1

or NT and with plasmids for empty vector (pCMV) or ATF6f along with the XBP1 luciferase reporter. CTL: sample transfected with NT and pCMV. Lower panel: western blot confirming the KD of GLI1 and the overexpression of ATF6f. β-Actin was used as loading control. **D)** Expression of the UPR target genes XBP1s and XBP1u following RT-qPCR analysis in U87 cells treated with siRNA control (NT) or siRNAs targeted towards GLI1 and exposed or not to Tun treatment (5 µg/ml for 24 h)**.** Blots presented are representative of three independent experiments. Results are represented as the average ± SEM of at least three independent experiments. *p<0.05; **p<0.01; ***p<0.001, ****p<0.0001.

Authors Contribution

Luciana L. Almada, Kim Barroso, Eric Chevet and Martin E. Fernandez-Zapico: conceptualization, methodology, experimentation, original draft preparation and writing. **Sandhya Sen, Murat Toruner, Ashley N. Sigafoos, Glancis L. Raja Arul, David R. Pease, Renzo E. Vera, and Rachel L. O. Olson**: experimentation, and data curation. **All:** reviewing and editing. **Eric Chevet and Martin E. Fernandez-Zapico:** funding acquisition.

CONFLICT OF INTEREST

The authors declare that they have no competing interests with the contents of this article.

Highlights

- p97/VCP is a novel transcriptional repressor of GLI1
- ER stress requires USF2 to antagonize a newly identified p97/VCP-HDAC1 complex to increases GLI1 expression
- GLI1 is a positive regulator of XBP1 expression under ER stress

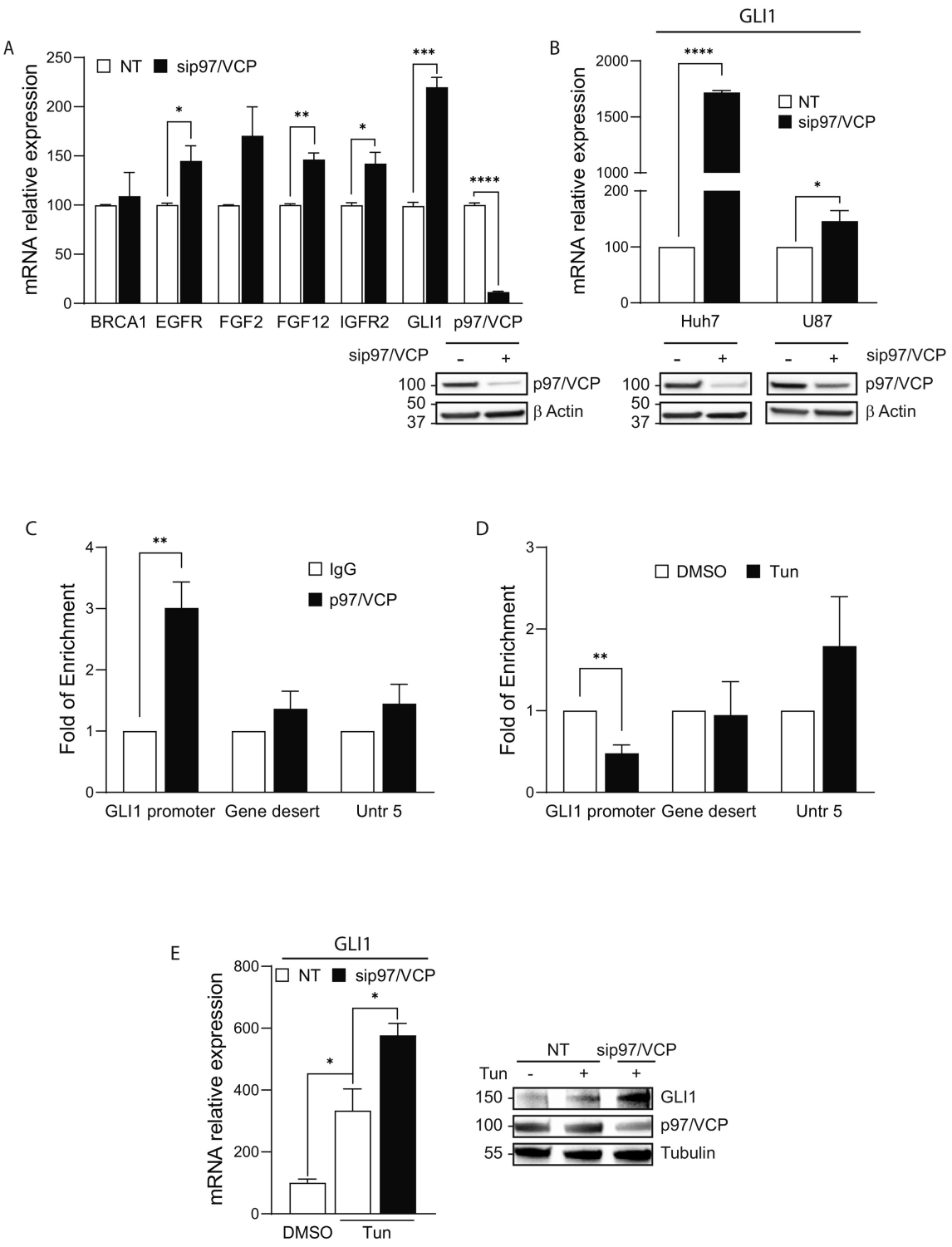
A
mRNA relative expression
NT
sip97/VCP
BRCA1
EGFR
FGF2
FGF12
IGFR2
GLI1
p97/VCP
sip97/VCP
p97/VCP
β Actin
B
GLI1
mRNA relative expression
NT
sip97/VCP
Huh7
U87
sip97/VCP
p97/VCP
β Actin
C
Fold of Enrichment
IgG
p97/VCP
GLI1 promoter
Gene desert
Untr 5
D
Fold of Enrichment
DMSO
Tun
GLI1 promoter
Gene desert
Untr 5
E
GLI1
mRNA relative expression
NT
sip97/VCP
DMSO
Tun
NT
sip97/VCP
Tun
GLI1
p97/VCP
Tubulin

Figure 1

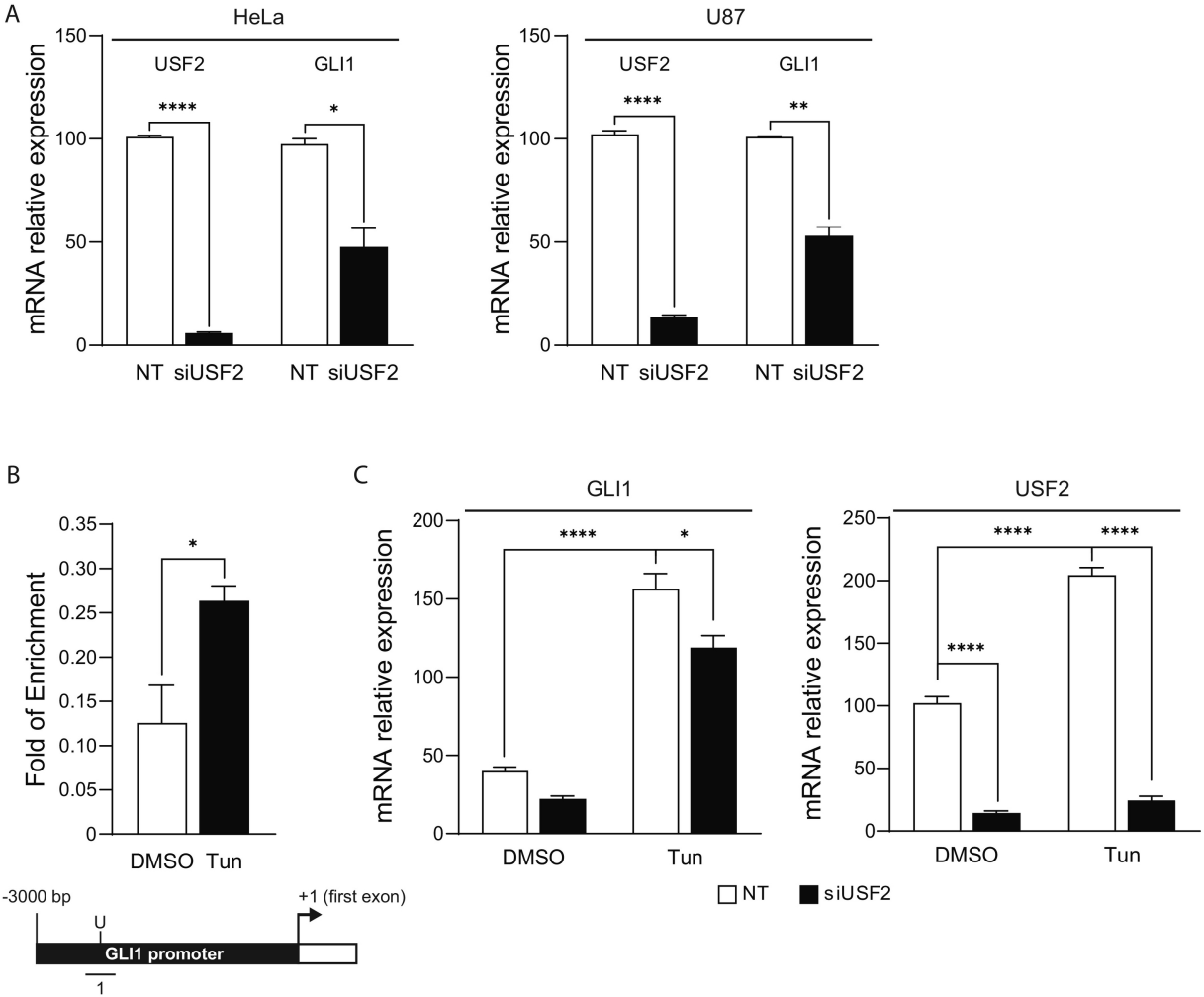
A
HeLa
U87
USF2
GLI1
mRNA relative expression
NT siUSF2
B
Fold of Enrichment
DMSO Tun
-3000 bp
+1 (first exon)
U
GLI1 promoter
1
C
GLI1
USF2
DMSO
Tun
NT
siUSF2

Figure 2

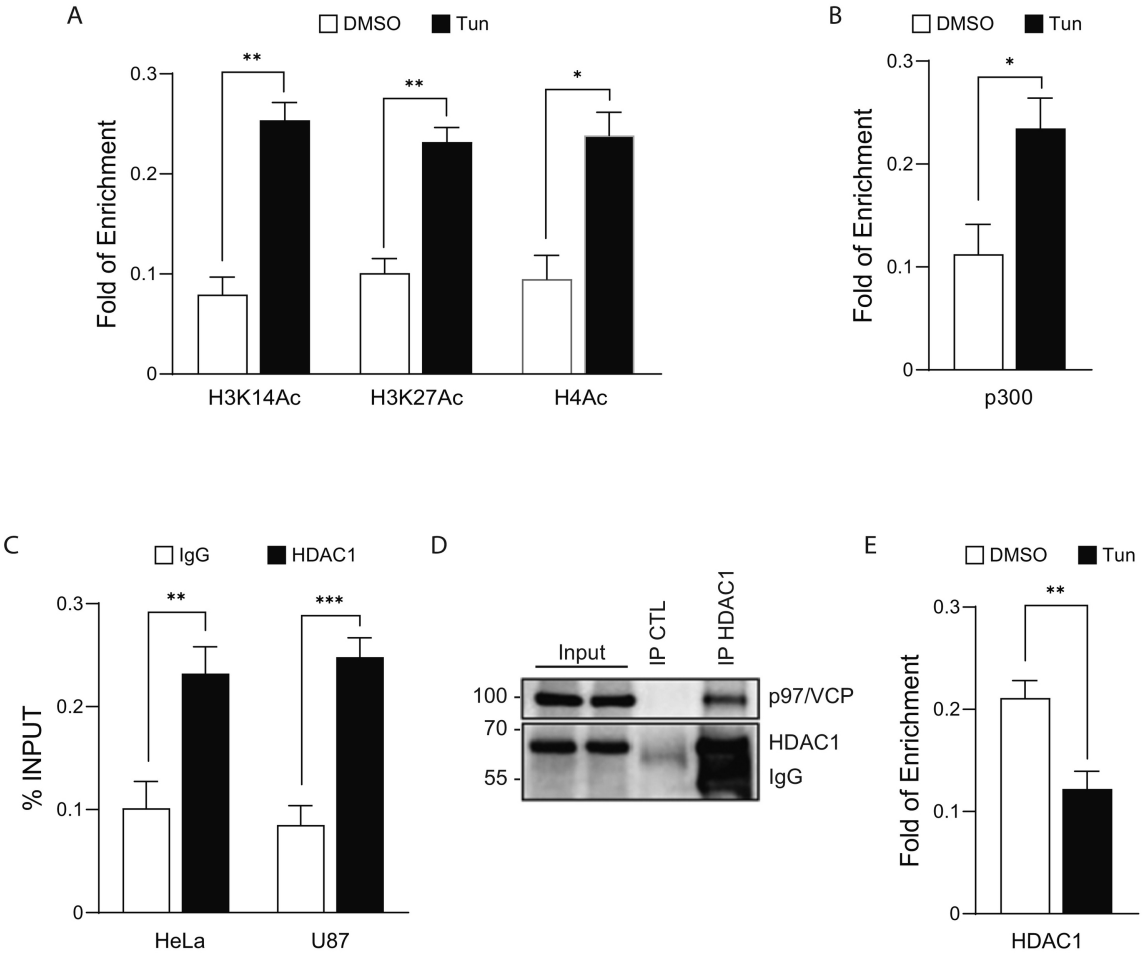
A
DMSO
Tun
Fold of Enrichment
0.3
0.2
0.1
0
**
**
*
H3K14Ac
H3K27Ac
H4Ac
B
DMSO
Tun
Fold of Enrichment
0.3
0.2
0.1
0
*
p300
C
IgG
HDAC1
% INPUT
0.3
0.2
0.1
0
**
***
HeLa
U87
D
Input
IP CTL
IP HDAC1
100
70
55
p97/VCP
HDAC1
IgG
E
DMSO
Tun
Fold of Enrichment
0.3
0.2
0.1
0
**
HDAC1

Figure 3

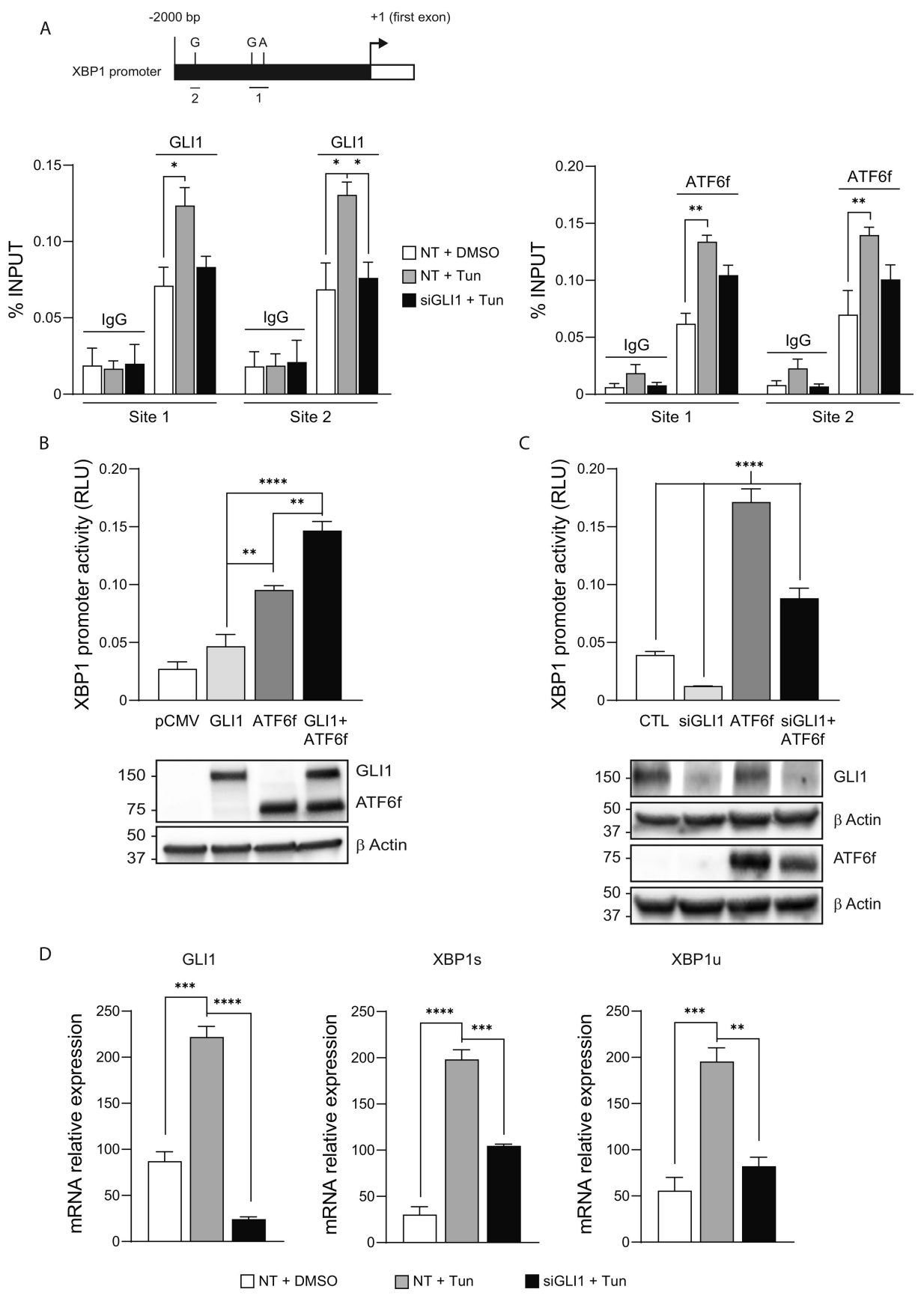
A
-2000 bp
+1 (first exon)
G
GA
XBP1 promoter
2
1
GLI1
GLI1
% INPUT
IgG
IgG
Site 1
Site 2
NT + DMSO
NT + Tun
siGLI1 + Tun
ATF6f
ATF6f
B
XBP1 promoter activity (RLU)
pCMV
GLI1
ATF6f
GLI1+ ATF6f
GLI1
ATF6f
β Actin
C
CTL
siGLI1
ATF6f
siGLI1+ ATF6f
GLI1
β Actin
ATF6f
β Actin
D
GLI1
XBP1s
XBP1u
mRNA relative expression
NT + DMSO
NT + Tun
siGLI1 + Tun

Figure 4